Spin-Orbit-Torque Switching of Ferrimagnets by Terahertz Electrical Pulses

Hao Wu,[1,2,*] Deniz Turan,[2] Quanjun Pan,[2] Chao-Yao Yang,[3,4] Guanjie Wu,[5] Seyed Armin Razavi,[2] Bingqian Dai,[2] Nezih Tolga Yardimci,[2] Zhi Huang,[1] Jing Zhang,[1] Yi-Ying Chin,[6] Hong-Ji Lin,[7] Chih-Huang Lai,[3] Zongzhi Zhang,[5] Mona Jarrahi,[2] and Kang L. Wang[2,†]

[1] *Songshan Lake Materials Laboratory, Dongguan, Guangdong 523808, China*

[2] *Department of Electrical and Computer Engineering, University of California, Los Angeles, California 90095, USA*

[3] *Department of Materials Science and Engineering, National Tsing Hua University, Hsinchu 30013, Taiwan*

[4] *Department of Materials Science and Engineering, National Yang Ming Chiao Tung University, Hsinchu 30013, Taiwan*

[5] *Shanghai Engineering Research Center of Ultra-Precision Optical Manufacturing, Department of Optical Science and Engineering, Fudan University, Shanghai 200433, China*

[6] *Department of Physics, National Chung Cheng University, Chiayi 621301, Taiwan*

[7] *National Synchrotron Radiation Research Center, Hsinchu 30076, Taiwan*

(Received 30 July 2022; revised 17 October 2022; accepted 27 October 2022; published 5 December 2022)

In conventional spintronic devices, ferromagnetic materials are used, which have a magnetization dynamics timescale of around nanoseconds, setting a limit for the switching speed. Increasing the magnetization switching speed has been one of the major challenges for spintronic research. In this work we take advantage of the ultrafast magnetic dynamics in ferrimagnetic materials instead of ferromagnets, and we use femtosecond laser pulses and a plasmonic photoconductive switch to create THz electrical pulses for ferrimagnetic switching by spin-orbit torque. By anomalous Hall and magneto-optic Kerr effect (MOKE) measurement, we demonstrate the robust THz-electrical-pulse-driven magnetization switching of ferrimagnetic Gd-Fe-Co. The time-resolved MOKE shows more than 50-GHz magnetic resonance frequency of Gd-Fe-Co, indicating faster than 20-ps magnetic dynamics. X-ray magnetic circular dichroism demonstrates the antiferromagnetically coupled Fe and Gd sublattices. Our work provides a promising route to realize ultrafast operation speed for nonvolatile magnetic memory and logic applications.

DOI: 10.1103/PhysRevApplied.18.064012

I. INTRODUCTION

Spintronics provides an efficient platform for realizing nonvolatile memory and logic applications [1,2]. In these systems, data are stored in the magnetization of magnetic materials, and the magnetization can be switched electrically in the writing process. Electrical manipulation of the magnetization is both fundamentally interesting and practically important for spintronic devices [3,4]. To date, two crucial issues need to be addressed: (1) reducing the energy consumption [5] and (2) increasing the switching speed [6]. There have been several approaches to reduce energy consumption, such as voltage-controlled magnetization [7–9], giant spin-orbit torque (SOT) in topological insulators [10–16], and so on. As for the switching speed, up to now, most spintronic devices are still operated on a timescale of several nanoseconds, which corresponds to the GHz magnetic resonance frequency of ferromagnetic materials. Ferrimagnets have antiferromagnetically (AFM) coupled spin sublattices; as a result, the AFM exchange coupling-induced magnetic resonance frequency is of the order of 100 GHz near the compensation point [17], which can achieve ultrafast magnetization switching speed [18–24].

There have been efforts for realizing ultrafast all-optical switching of ferrimagnetic materials [25], with circularly polarized femtosecond laser pulses resulting in a switching speed of the order of tens of picoseconds [26–29]. Similarly, laser-induced hot-electron pulses have been exploited to induce ultrafast switching dynamics in ferrimagnetic materials [30–32]. However, these methods mainly rely on heating effects and have a relatively low energy efficiency compared to electrical methods. Therefore, ultrafast electrical switching of ferrimagnets provides a promising route with a high energy efficiency. A recent work has demonstrated 6-ps electrical-pulse-induced magnetization switching in a ferromagnetic Co film [33]; however, ultrafast ferrimagnetic switching with

*wuhao1@sslab.org.cn
†wang@ee.ucla.edu

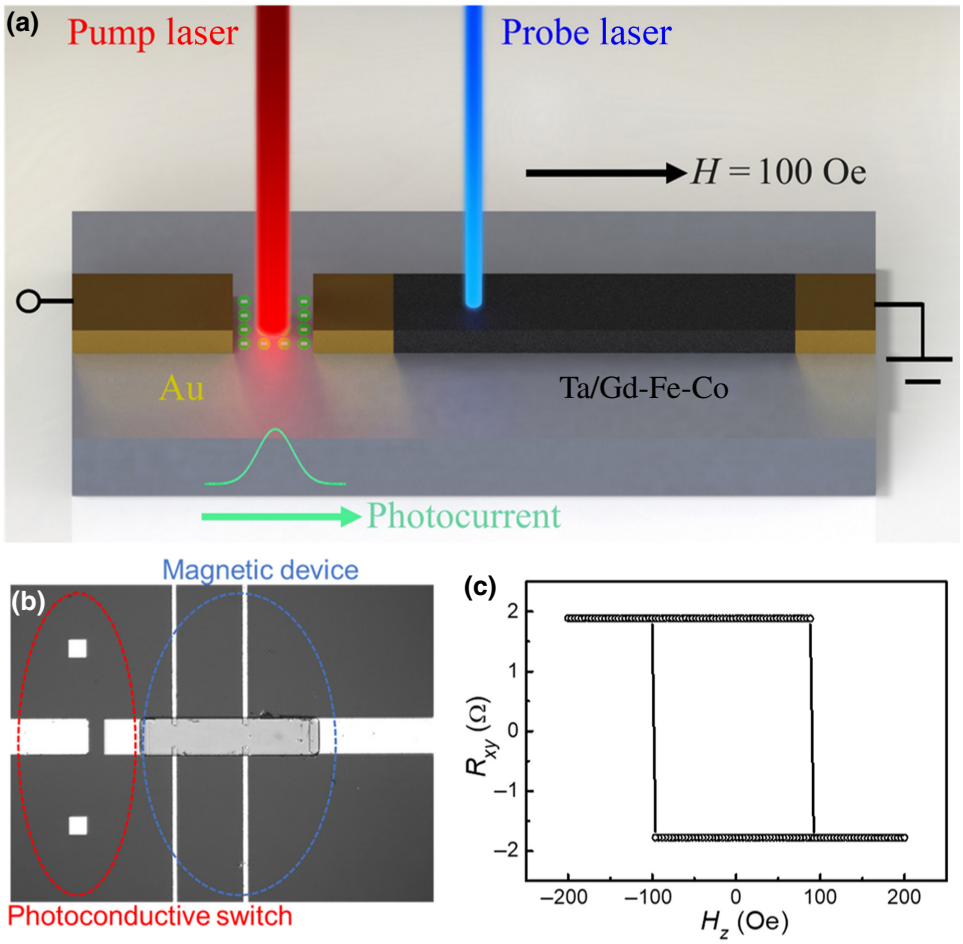

FIG. 1. (a) Schematic of the plasmonic photoconductive switch + magnetic strip device and the measurement setup. Femtosecond laser pulses are focused on the gap of the voltage-biased photoconductive switch to excite picosecond electrical currents, which then provide ultrafast SOT on the ferrimagnetic Gd-Fe-Co. (b) Scanning electron microscope image of the patterned plasmonic photoconductive switch + magnetic strip device. (c) R_{xy}–H_z curve shows the strong perpendicular magnetic anisotropy of Gd-Fe-Co.

much faster AFM-type magnetic dynamics is still waiting to be discovered.

In this work, a plasmonic photoconductive switch is employed to generate THz electrical pulses by femtosecond (150–200 fs) laser pulses [34], which is used to provide ultrafast SOT switching [35–39] in Ta/Gd-Fe-Co heterostructures. The magnetization switching is detected by both the anomalous Hall effect (AHE) and the magneto-optic Kerr effect (MOKE), which demonstrate the robust magnetization switching by the ultrafast SOT, with a peak current density of 10^7 A/cm^2. Furthermore, more than 50-GHz magnetic dynamics of Gd-Fe-Co is detected by the time-resolved MOKE (TR MOKE), further confirming the ultrafast magnetic dynamics of ferrimagnets. The AFM-coupled Fe and Gd sublattices are detected by x-ray magnetic circular dichroism (XMCD).

II. EXPERIMENTAL DETAILS AND RESULTS

Figure 1(a) shows a schematic of the device structure and the measurement method, where a plasmonic photoconductive switch is connected to a magnetic strip of a Ta(5)/Gd-Fe-Co(6)/MgO(2)/Ta(2) (thickness in nanometers) heterostructure. $Gd_{24}(FeCo)_{76}$ is prepared by the cosputtering method of Gd and FeCo targets, with CoFe-rich magnetization at room temperature. When the femtosecond laser pulses are focused on the gap of the photoconductive switch, the charge carriers are excited in the conduction band of low-temperature-grown GaAs, which are subsequently accelerated by the bias voltage (10 V). Based upon simulations in the Sentaurus software package, the induced photocurrent response time is estimated to be around 1 ps [40]. The magnetization of Gd-Fe-Co is detected by either the AHE or the MOKE, where an in-plane magnetic field is applied to break the inversion symmetry between $\pm M$ for the deterministic SOT switching. Figure 1(b) shows a microscopic image of the photoconductive switch + magnetic strip device, where the width of the magnetic strip is 20 μm. The R_{xy}–H_z curve in Fig. 1(c) demonstrates the strong perpendicular magnetic anisotropy of Gd-Fe-Co.

To test the device, we first perform all-electrical SOT switching of the Ta/Gd-Fe-Co heterostructure by using relatively long electrical pulses. Figures 2(a) and 2(b) show the current-driven SOT switching, where the magnetization is detected by the AHE resistance. In this measurement scheme, a 1-ms writing current pulse is applied to the switch the magnetization firstly, which is followed one

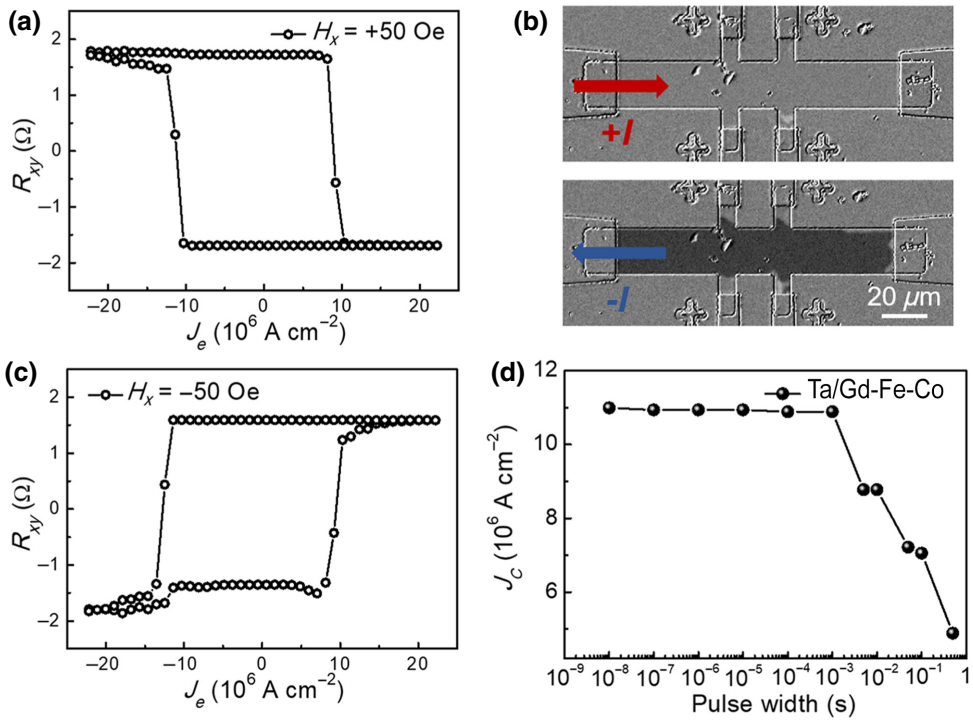

FIG. 2. Current-driven SOT switching of the Ta/Gd-Fe-Co heterostructure under (a) $H_x = +50$ Oe and (b) $H_x = -50$ Oe. (c) SOT-driven magnetic domain switching measured by the MOKE microscope. (d) Switching current density J_c as a function of the pulse width of the writing current.

second later by another 1-ms reading current pulse to detect the AHE resistance. Under ±50-Oe in-plane magnetic field H_x, the current-induced switching polarity changes, which is a typical SOT characteristic. The switching current density J_c is around 1.1×10^7 A/cm^2 for the 1-ms writing pulse, which is similar to that of previous reports [22,41,42]. MOKE microscope is employed to detect the magnetic domain directly, which also clearly shows the robust SOT-driven magnetic domain switching, as shown in Fig. 2(c). In order to figure out the current-induced Joule heating effect on the SOT switching, we change the writing pulse width from 0.5 s to 10 ns, as shown in Fig. 2(d). J_c significantly increases for the writing pulse width from 0.5 s to 1 ms, and then slightly changes from 1 ms to 10 ns, indicating Joule heating is not a dominant effect with shorter writing pulses.

The magnetic precession period (tens of picoseconds) of the Gd-Fe-Co samples is more than 2 orders of magnitude shorter than the duration time of the writing pulses in Fig. 2(d) [17]. It is therefore reasonable to expect that the SOT switching of Gd-Fe-Co could be achieved in devices subjected to significantly shorter writing pulses. Previous time-resolved magnetization studies of Gd-Fe-Co structures report full magnetization switching in structures subjected to picosecond-length optical excitation [25–32]. However, these previous results are both rooted in thermal effects; therefore, the demonstration of deterministic, ultrafast, and electrical switching of Gd-Fe-Co magnetization is highly desirable from a technological perspective.

To test the temporal limitations of SOT switching in the Ta/Gd-Fe-Co heterostructure, we perform experiments on devices subjected to picosecond-duration electrical pulses. These ultrashort electrical excitations are generated by illuminating a dc biased photoconductive switch with the femtosecond output of a mode-locked Ti:sapphire laser. A typical device used for these experiments is depicted in Fig. 1(b). Given the duration of the laser pulse (approximately 150 fs) and the known carrier lifetime within the switch (approximately 300 fs), electrical pulses of the order of 1-ps duration are predicted by simulations in the Sentaurius software package. By tuning the applied laser power (100 mW) and the bias voltage (10 V), average currents as high as 10 μA are observed in these devices, equating to a peak density of 10^7 A/cm^2 for picosecond currents. When testing the viability of ultrafast SOT switching in our devices, we apply an in-plane magnetic field to the device under test to break the inversion symmetry between $\pm M$. Experiments are performed by illuminating the switch for approximately 1 minute, and then reading out the magnetization state through measurements of the AHE resistance [Fig. 3(a)] and the Kerr rotation angle [Fig. 3(b)]. Significantly, we observe that the magnetization states of the

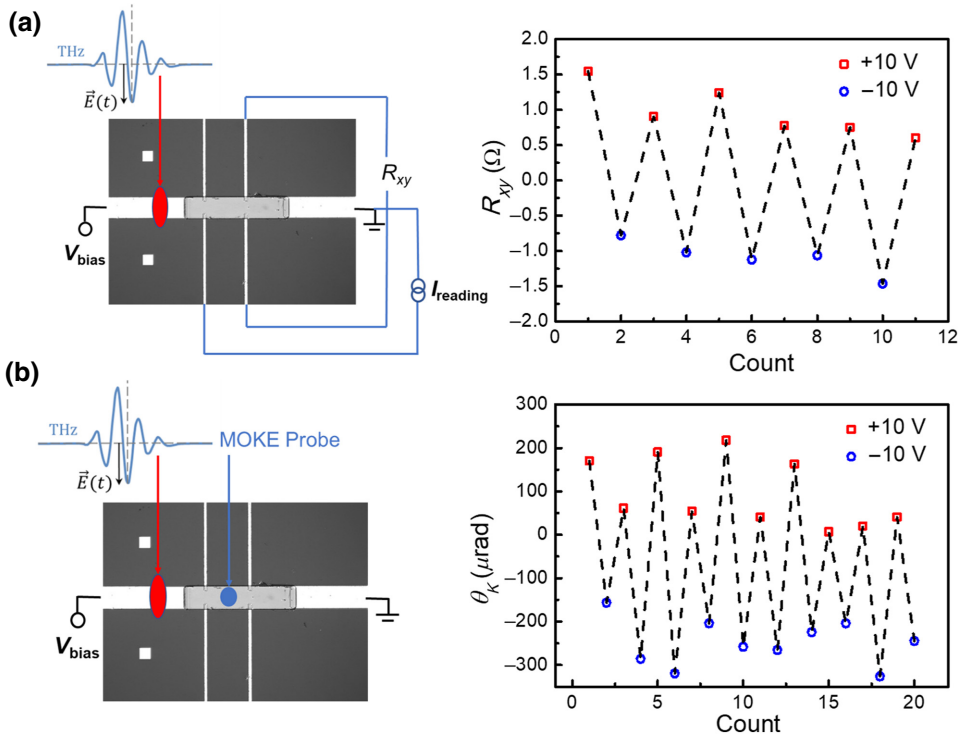

FIG. 3. (a) Femtosecond laser pulses are applied at the gap of the plasmonic photoconductive switch to excite picosecond (THz) electrical current pulses under bias voltage, and then provide an ultrafast SOT on the Ta/Gd-Fe-Co heterostructure, where the magnetization is detected by AHE resistance. When the bias voltage polarity is switched between +10 V and −10 V, the sign change of the AHE resistance demonstrates the magnetization switching between up and down states, which indicates the SOT switching rather than thermal-induced switching. (b) THz-electrical-pulse-driven magnetization switching detected by the MOKE method.

device are indeed switched when subject to this procedure. We observe that the final magnetization state of our devices is dependent upon the polarity of the bias voltage across the switch, as shown in Figs. 3(a) and 3(b), indicating that this magnetization switching primarily comes from THz-electrical-current-induced SOT, rather than as a consequence of thermal effects.

While deterministic switching is observed in our ultrafast measurements, the measured Hall and Kerr signals provided in Figs. 3(a) and 3(b) do not fully return to their initial state upon magnetization reversal, and appear to drift slightly over many switching cycles. The failure to recover the Hall resistivity and Kerr rotation observed at full magnetization is likely an indicator of only partial SOT switching in these devices, resulting in a multidomain final state. That the Hall resistance and Kerr rotation of the final state drift following several switching cycles stems from an asymmetry in the current generated in our

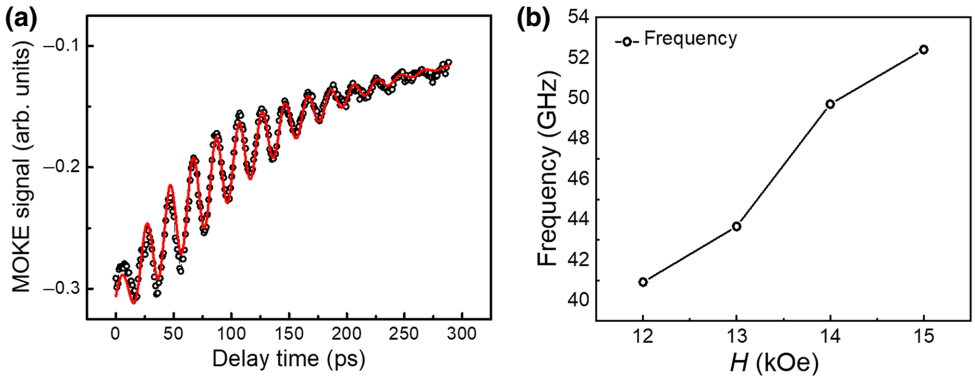

FIG. 4. (a) Normalized dynamic TR-MOKE signals for the Ta/Gd-Fe-Co heterostructure. (b) Magnetic resonance frequency as a function of the magnetic field.

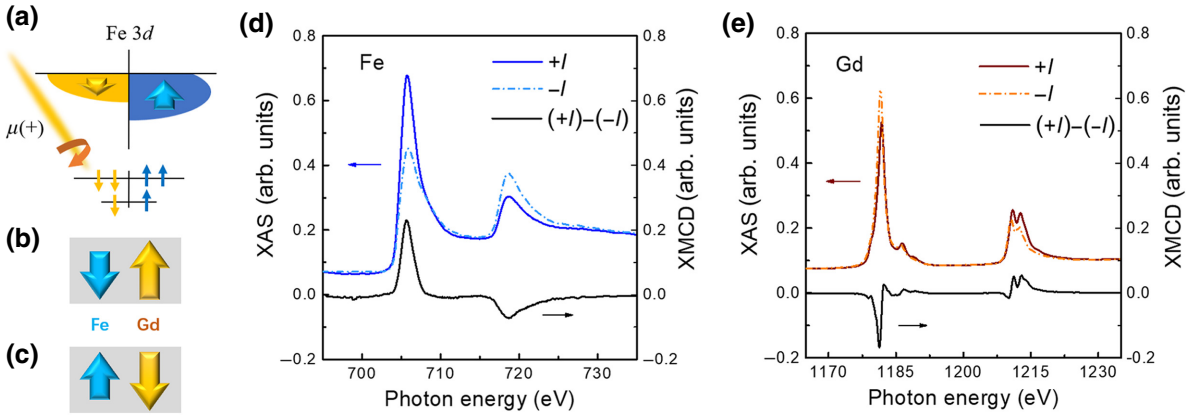

FIG. 5. Probing magnetic states of Fe and Gd by using element-specific XMCD. (a) Scheme of spin-dependent absorption excited by circularly polarized x-rays. $\mu(+)$ represents right-handed circularly polarized x rays, triggering excitation for spin down. Ferrimagnetic coupling between Fe and Gd with net magnetization (b) downward and (c) upward treated by SOT. (d) XAS signals at Fe L_3 and L_2 edges acquired from the magnetic states corresponding to (b),(c) along with the XMCD gained by the difference between these two XAS signals. (e) XAS signals at Gd M_5 and M_4 edges acquired from the magnetic states corresponding to (b),(c) along with the XMCD gained by the difference between these two XAS signals. The x-ray absorption spectra in (d),(e) are all acquired with fixed x-ray helicity $\mu(+)$.

photoconductive switch upon the reversal of the external bias.

We show that THz electrical pulses can efficiently switch the ferrimagnetic Gd-Fe-Co, while another important question is how fast is the magnetization switching speed? In order to answer this question, we perform TR-MOKE measurements [43–45] to pick up the magnetic dynamics of the ferrimagnetic Gd-Fe-Co: an optical pump laser pulse is applied to excite the magnetic dynamics of a Gd-Fe-Co blanket film by the ultrafast demagnetization and recovery process, and the probe laser is followed to detect the spin state of Gd-Fe-Co with a time delay. By changing the delay time between pump and probe laser pulses, we can get the time-resolved magnetic dynamics of Gd-Fe-Co, i.e., TR MOKE. Figure 4(a) shows a typical TR-MOKE curve of the Ta/Gd-Fe-Co heterostructure under $H = 15$ kOe. To extract precession frequency f, the dynamic Kerr signals are fitted by using the following expression [46]:

$$\theta_k = c_0 + c_1 \exp(t/t_0) + c_2 \sin(2\pi f t + \varphi) \exp(-t/\tau), \tag{1}$$

where c_0 is the background signal. The second term is an exponential decaying signal representing the slow recovery process, where c_1 is the amplitude and t_0 is the characteristic relaxation time. c_2, f, φ, and τ in the third term represent the magnetization precession parameters of amplitude, frequency, initial phase, and decay time, respectively. The fitted frequencies under different H are shown in Fig. 4(b), which is consistent with our expectations. From the fitting, we can get a magnetic resonance frequency of Gd-Fe-Co of as large as 52.4 GHz, which corresponds to a faster than 20-ps timescale of magnetic dynamics.

In order to monitor the AFM-coupled sublattice switching, we perform element-specific x-ray absorption spectroscopy (XAS) [47,48] [schematically shown in Figs. 5(a)–5(c)], which covers the Fe L_3 and L_2 absorption edges [Fig. 5(d)] and the Gd M_5 and M_4 edges [Fig. 5(e)] with a fixed x-ray helicity $\mu(+)$ and varying SOT current polarities ($\pm 2.0 \times 10^7$ A/cm^2). The appearance of XMCD for Fe and Gd acquired by their XAS difference triggered by 1-ms current pulses $\pm I$ suggests the current (SOT)-induced spontaneous magnetization switching of Fe and Gd sublattices. The current-driven XMCD signals clearly show the AFM-coupled SOT switching for Fe and Gd sublattices in the ferrimagnetic Gd-Fe-Co in terms of the opposite sign of Fe and Gd XMCD. A sum-rule calculation is performed to quantitatively verify the atomic moments of Fe and Gd, which are $2.1\mu_B$ and $2.36\mu_B$, respectively. The results are very close to the reported values for Fe and Gd [49,50], suggesting the complete switching of the two sublattices.

III. CONCLUSION

In summary, by combing a plasmonic photoconductive switch with a Ta/Gd-Fe-Co heterostructure, THz electrical pulses are applied to provide ultrafast SOT, where both AHE and MOKE measurements demonstrate the robust ultrafast SOT-induced magnetization switching. The TR-MOKE measurement demonstrates a more than 50-GHz magnetic resonance frequency, indicating the ultrafast magnetic dynamics of ferrimagnetic Gd-Fe-Co. XMCD signals detect the AFM-coupled sublattice (Fe and Gd) switching of ferrimagnetic Gd-Fe-Co. These results demonstrate the THz-electrical-pulse-driven

magnetization switching of ferrimagnets, with great potential for future ultrafast spintronic applications.

ACKNOWLEDGMENTS

This work is supported by the National Key Research and Development Program (Grant No. 2022YFA1402801), the National Natural Science Foundation of China (NSFC) (Grant No. 52271239), start-up funding from Songshan Lake Materials Laboratory (Grant No. Y1D1071S511), NSF Awards No. 1935362, No. 1909416, No. 1810163, and No. 1611570, the Nanosystems Engineering Research Center for Translational Applications of Nanoscale Multiferroic Systems (TANMS), and the U.S. Army Research Office MURI program under Grants No. W911NF-16-1-0472 and No. WN911NF-20-2-0166. G.W. and Z.Z. are supported by the NSFC (Grants No. 11874120 and No. 51671057).

[1] I. Žutić, J. Fabian, and S. Das Sarma, Spintronics: Fundamentals and applications, Rev. Mod. Phys. **76**, 323 (2004).

[2] S. A. Wolf, D. D. Awschalom, R. A. Buhrman, J. M. Daughton, S. von Molnár, M. L. Roukes, A. Y. Chtchelkanova, and D. M. Treger, Spintronics: A spin-based electronics vision for the future, Science **294**, 1488 (2001).

[3] E. B. Myers, D. C. Ralph, J. A. Katine, R. N. Louie, and R. A. Buhrman, Current-induced switching of domains in magnetic multilayer devices, Science **285**, 867 (1999).

[4] J. C. Slonczewski, Current-driven excitation of magnetic multilayers, J. Magn. Magn. Mater. **159**, L1 (1996).

[5] K. L. Wang, H. Wu, S. A. Razavi, and Q. Shao, in *2018 IEEE International Electron Devices Meeting (IEDM)* (2018), pp. 36.32.31–36.32.34.

[6] G. Beach, Beyond the speed limit, Nat. Mater. **9**, 959 (2010).

[7] T. Maruyama, Y. Shiota, T. Nozaki, K. Ohta, N. Toda, M. Mizuguchi, A. A. Tulapurkar, T. Shinjo, M. Shiraishi, S. Mizukami, *et al.*, Large voltage-induced magnetic anisotropy change in a few atomic layers of iron, Nat. Nanotechnol. **4**, 158 (2009).

[8] X. Li, A. Lee, S. A. Razavi, H. Wu, and K. L. Wang, Voltage-controlled magnetoelectric memory and logic devices, MRS Bull. **43**, 970 (2018).

[9] W.-G. Wang, M. Li, S. Hageman, and C. L. Chien, Electric-field-assisted switching in magnetic tunnel junctions, Nat. Mater. **11**, 64 (2012).

[10] Y. Fan, P. Upadhyaya, X. Kou, M. Lang, S. Takei, Z. Wang, J. Tang, L. He, L.-T. Chang, M. Montazeri, *et al.*, Magnetization switching through giant spin–orbit torque in a magnetically doped topological insulator heterostructure, Nat. Mater. **13**, 699 (2014).

[11] J. Han, A. Richardella, S. A. Siddiqui, J. Finley, N. Samarth, and L. Liu, Room-Temperature Spin-Orbit Torque Switching Induced by a Topological Insulator, Phys. Rev. Lett. **119**, 077702 (2017).

[12] M. Dc, R. Grassi, J.-Y. Chen, M. Jamali, D. Reifsnyder Hickey, D. Zhang, Z. Zhao, H. Li, P. Quarterman, Y. Lv, *et al.*, Room-temperature high spin–orbit torque due to quantum confinement in sputtered $Bi_xSe_{(1-x)}$ films, Nat. Mater. **17**, 800 (2018).

[13] N. H. D. Khang, Y. Ueda, and P. N. Hai, A conductive topological insulator with large spin Hall effect for ultralow power spin–orbit torque switching, Nat. Mater. **17**, 808 (2018).

[14] H. Wu, P. Zhang, P. Deng, Q. Lan, Q. Pan, S. A. Razavi, X. Che, L. Huang, B. Dai, K. Wong, *et al.*, Room-Temperature Spin-Orbit Torque from Topological Surface States, Phys. Rev. Lett. **123**, 207205 (2019).

[15] H. Wu, Y. Xu, P. Deng, Q. Pan, S. A. Razavi, K. Wong, L. Huang, B. Dai, Q. Shao, G. Yu, *et al.*, Spin-orbit torque switching of a nearly compensated ferrimagnet by topological surface states, Adv. Mater. **31**, 1901681 (2019).

[16] H. Wu, *et al.*, Magnetic memory driven by topological insulators, Nat. Commun. **12**, 6251 (2021).

[17] C. D. Stanciu, A. V. Kimel, F. Hansteen, A. Tsukamoto, A. Itoh, A. Kirilyuk, and T. Rasing, Ultrafast spin dynamics across compensation points in ferrimagnetic GdFeCo: The role of angular momentum compensation, Phys. Rev. B **73**, 220402 (2006).

[18] L. Caretta, M. Mann, F. Büttner, K. Ueda, B. Pfau, C. M. Günther, P. Hessing, A. Churikova, C. Klose, M. Schneider, *et al.*, Fast current-driven domain walls and small skyrmions in a compensated ferrimagnet, Nat. Nanotechnol. **13**, 1154 (2018).

[19] R. Bläsing, T. Ma, S.-H. Yang, C. Garg, F. K. Dejene, A. T. N'Diaye, G. Chen, K. Liu, and S. S. P. Parkin, Exchange coupling torque in ferrimagnetic Co/Gd bilayer maximized near angular momentum compensation temperature, Nat. Commun. **9**, 4984 (2018).

[20] C. O. Avci, E. Rosenberg, L. Caretta, F. Büttner, M. Mann, C. Marcus, D. Bono, C. A. Ross, and G. S. D. Beach, Interface-driven chiral magnetism and current-driven domain walls in insulating magnetic garnets, Nat. Nanotechnol. **14**, 561 (2019).

[21] S. Vélez, J. Schaab, M. S. Wörnle, M. Müller, E. Gradauskaite, P. Welter, C. Gutgsell, C. Nistor, C. L. Degen, M. Trassin, *et al.*, High-speed domain wall racetracks in a magnetic insulator, Nat. Commun. **10**, 4750 (2019).

[22] K. Cai, Z. Zhu, J. M. Lee, R. Mishra, L. Ren, S. D. Pollard, P. He, G. Liang, K. L. Teo, and H. Yang, Ultrafast and energy-efficient spin–orbit torque switching in compensated ferrimagnets, Nat. Electron. **3**, 37 (2020).

[23] G. Sala, V. Krizakova, E. Grimaldi, C. H. Lambert, T. Devolder, and P. Gambardella, Real-time Hall-effect detection of current-induced magnetization dynamics in ferrimagnets, Nat. Commun. **12**, 656 (2021).

[24] G. Sala, C.-H. Lambert, S. Finizio, V. Raposo, V. Krizakova, G. Krishnaswamy, M. Weigand, J. Raabe, M. D. Rossell, E. Martinez, and P. Gambardella, Asynchronous current-induced switching of rare-earth and transition-metal sublattices in ferrimagnetic alloys, Nat. Mater. **21**, 640 (2022).

[25] A. Kirilyuk, A. V. Kimel, and T. Rasing, Ultrafast optical manipulation of magnetic order, Rev. Mod. Phys. **82**, 2731 (2010).

[26] C. D. Stanciu, F. Hansteen, A. V. Kimel, A. Kirilyuk, A. Tsukamoto, A. Itoh, and T. Rasing, All-Optical Magnetic

Recording with Circularly Polarized Light, Phys. Rev. Lett. **99**, 047601 (2007).

[27] A. V. Kimel, A. Kirilyuk, P. A. Usachev, R. V. Pisarev, A. M. Balbashov, and T. Rasing, Ultrafast non-thermal control of magnetization by instantaneous photomagnetic pulses, Nature **435**, 655 (2005).

[28] C.-H. Lambert, S. Mangin, B. S. D. C. S. Varaprasad, Y. K. Takahashi, M. Hehn, M. Cinchetti, G. Malinowski, K. Hono, Y. Fainman, M. Aeschlimann, and E. E. Fullerton, All-optical control of ferromagnetic thin films and nanostructures, Science **345**, 1337 (2014).

[29] S. Mangin, M. Gottwald, C. H. Lambert, D. Steil, V. Uhlíř, L. Pang, M. Hehn, S. Alebrand, M. Cinchetti, G. Malinowski, *et al.*, Engineered materials for all-optical helicity-dependent magnetic switching, Nat. Mater. **13**, 286 (2014).

[30] Y. Xu, M. Deb, G. Malinowski, M. Hehn, W. Zhao, and S. Mangin, Ultrafast magnetization manipulation using single femtosecond light and hot-electron pulses, Adv. Mater. **29**, 1703474 (2017).

[31] Y. Yang, R. B. Wilson, J. Gorchon, C.-H. Lambert, S. Salahuddin, and J. Bokor, Ultrafast magnetization reversal by picosecond electrical pulses, Sci. Adv. **3**, e1603117 (2017).

[32] I. Radu, K. Vahaplar, C. Stamm, T. Kachel, N. Pontius, H. A. Dürr, T. A. Ostler, J. Barker, R. F. L. Evans, R. W. Chantrell, *et al.*, Transient ferromagnetic-like state mediating ultrafast reversal of antiferromagnetically coupled spins, Nature **472**, 205 (2011).

[33] K. Jhuria, J. Hohlfeld, A. Pattabi, E. Martin, A. Y. Arriola Córdova, X. Shi, R. Lo Conte, S. Petit-Watelot, J. C. Rojas-Sanchez, G. Malinowski, *et al.*, Spin–orbit torque switching of a ferromagnet with picosecond electrical pulses, Nat. Electron. **3**, 680 (2020).

[34] C. W. Berry, N. Wang, M. R. Hashemi, M. Unlu, and M. Jarrahi, Significant performance enhancement in photoconductive terahertz optoelectronics by incorporating plasmonic contact electrodes, Nat. Commun. **4**, 1622 (2013).

[35] I. M. Miron, K. Garello, G. Gaudin, P.-J. Zermatten, M. V. Costache, S. Auffret, S. Bandiera, B. Rodmacq, A. Schuhl, and P. Gambardella, Perpendicular switching of a single ferromagnetic layer induced by in-plane current injection, Nature **476**, 189 (2011).

[36] L. Liu, O. J. Lee, T. J. Gudmundsen, D. C. Ralph, and R. A. Buhrman, Current-Induced Switching of Perpendicularly Magnetized Magnetic Layers Using Spin Torque from the Spin Hall Effect, Phys. Rev. Lett. **109**, 096602 (2012).

[37] L. Liu, C.-F. Pai, Y. Li, H. W. Tseng, D. C. Ralph, and R. A. Buhrman, Spin-torque switching with the giant spin Hall effect of tantalum, Science **336**, 555 (2012).

[38] A. Manchon, J. Železný, I. M. Miron, T. Jungwirth, J. Sinova, A. Thiaville, K. Garello, and P. Gambardella, Current-induced spin-orbit torques in ferromagnetic and antiferromagnetic systems, Rev. Mod. Phys. **91**, 035004 (2019).

[39] Q. Shao, P. Li, L. Liu, H. Yang, S. Fukami, A. Razavi, H. Wu, K. Wang, F. Freimuth, Y. Mokrousov, *et al.*, Roadmap of spin–orbit torques, IEEE Trans. Magn. **57**, 1 (2021).

[40] See Supplemental Material at http://link.aps.org/supplemental/10.1103/PhysRevApplied.18.064012 for materials and methods, temporal profile of the photocurrent with Sentaurus simulations, and scanning electron microscopy images.

[41] N. Roschewsky, C.-H. Lambert, and S. Salahuddin, Spin-orbit torque switching of ultralarge-thickness ferrimagnetic GdFeCo, Phys. Rev. B **96**, 064406 (2017).

[42] H. Wu, J. Nance, S. A. Razavi, D. Lujan, B. Dai, Y. Liu, H. He, B. Cui, D. Wu, K. Wong, *et al.*, Chiral symmetry breaking for deterministic switching of perpendicular magnetization by spin–orbit torque, Nano Lett. **21**, 515 (2021).

[43] G. Ju, A. V. Nurmikko, R. F. C. Farrow, R. F. Marks, M. J. Carey, and B. A. Gurney, Ultrafast Time Resolved Photoinduced Magnetization Rotation in a Ferromagnetic/Antiferromagnetic Exchange Coupled System, Phys. Rev. Lett. **82**, 3705 (1999).

[44] M. van Kampen, C. Jozsa, J. T. Kohlhepp, P. LeClair, L. Lagae, W. J. M. de Jonge, and B. Koopmans, All-Optical Probe of Coherent Spin Waves, Phys. Rev. Lett. **88**, 227201 (2002).

[45] A. Mekonnen, M. Cormier, A. V. Kimel, A. Kirilyuk, A. Hrabec, L. Ranno, and T. Rasing, Femtosecond Laser Excitation of Spin Resonances in Amorphous Ferrimagnetic $Gd_{1-x}Co_x$ Alloys, Phys. Rev. Lett. **107**, 117202 (2011).

[46] G. Wu, S. Chen, Y. Ren, Q. Y. Jin, and Z. Zhang, Laser-induced magnetization dynamics in interlayer-coupled $[Ni/Co]_4/Ru/[Co/Ni]_3$ perpendicular magnetic films for information storage, ACS Appl. Nano Mater. **2**, 5140 (2019).

[47] J. Stöhr, Exploring the microscopic origin of magnetic anisotropies with x-ray magnetic circular dichroism (XMCD) spectroscopy, J. Magn. Magn. Mater. **200**, 470 (1999).

[48] H. Wu, F. Groß, B. Dai, D. Lujan, S. A. Razavi, P. Zhang, Y. Liu, K. Sobotkiewich, J. Förster, M. Weigand, *et al.*, Ferrimagnetic skyrmions in topological insulator/ferrimagnet heterostructures, Adv. Mater. **32**, 2003380 (2020).

[49] C. W. Chuang, H. J. Lin, F. M. F. de Groot, F. H. Chang, C. T. Chen, Y. Y. Chin, Y. F. Liao, K. D. Tsuei, J. A. Chelvane, R. Nirmala, and A. Chainani, Electronic structure investigation of GdNi using x-ray absorption, magnetic circular dichroism, and hard x-ray photoemission spectroscopy, Phys. Rev. B **101**, 115137 (2020).

[50] C. T. Chen, Y. U. Idzerda, H. J. Lin, N. V. Smith, G. Meigs, E. Chaban, G. H. Ho, E. Pellegrin, and F. Sette, Experimental Confirmation of the X-Ray Magnetic Circular Dichroism Sum Rules for Iron and Cobalt, Phys. Rev. Lett. **75**, 152 (1995).